Journal of Dentistry 89 (2019) 103172

Contents lists available at ScienceDirect

Journal of Dentistry

journal homepage: www.elsevier.com/locate/jdent

A nano-CaF_2-containing orthodontic cement with antibacterial and remineralization capabilities to combat enamel white spot lesions

Jianru Yi[a,b], Quan Dai[b,c], Michael D. Weir[b], Mary A.S. Melo[b], Christopher D. Lynch[d], Thomas W. Oates[b], Ke Zhang[b,e,**], Zhihe Zhao[a,***], Hockin H.K. Xu[b,f,g,*]

[a] State Key Laboratory of Oral Diseases, National Clinical Research Center for Oral Diseases, Dept. of Orthodontic and Pediatric Dentistry, West China Hospital of Stomatology, Sichuan University, China
[b] Department of Advanced Oral Sciences and Therapeutics, School of Dentistry, University of Maryland, Baltimore, MD 21021, USA
[c] Clinical Research Center of Shaanxi Province for Dental and Maxillofacial Diseases, Key Laboratory of Shaanxi Province for Craniofacial Precision Medicine Research, Department of General Dentistry, College of Stomatology, Xi'an Jiaotong University, Xi'an, Shaanxi 710004, China
[d] Restorative Dentistry, University Dental School and Hospital, University College Cork, Wilton, Cork, Ireland
[e] School of Stomatology, Capital Medical University, Beijing, China
[f] Center for Stem Cell Biology & Regenerative Medicine, University of Maryland School of Medicine, Baltimore, MD, 21201, USA
[g] Marlene and Stewart Greenebaum Cancer Center, University of Maryland School of Medicine, Baltimore, MD, 21201, USA

ARTICLE INFO

Keywords:
Nano CaF_2
Orthodontic cement
Antibiofilm
Enamel hardness
Remineralization
White spot lesions

ABSTRACT

Objectives: The objectives of this study were to develop a resin-modified glass ionomer containing nanoparticles of calcium fluoride ($nCaF_2$) and dimethylaminohexadecyl methacrylate (DMAHDM) for the first time and investigate the antibacterial and remineralization properties.

Methods: $nCaF_2$ was synthesized using a spray-drying method and characterized using a transmission electron microscope. Twenty weight percentage (wt%) $nCaF_2$ and 3 wt% DMAHDM were incorporated into a RMGI (GC Ortho LC). Enamel shear bond strength (SBS) and cytotoxicity were determined. Fluoride (F) and calcium (Ca) ion releases were assessed. Biofilm live/dead staining, metabolic activity, polysaccharide and lactic production, and colony-forming units (CFU) were evaluated. The remineralization ability was determined by measuring the effects of cements on enamel surface hardness and lesion depth.

Results: Incorporating 20 wt% $nCaF_2$ and 3 wt% DMAHDM did not compromise the SBS ($p > 0.1$). The decrease of pH from 7.0 to 4.0 significantly increased the F and Ca ion releases. The new cement greatly reduced the metabolic activity, polysaccharide and lactic acid productions, and lowered the biofilm CFU by 3 log, compared to commercial control ($p < 0.05$). The new cement increased the enamel hardness by 56% and decreased the lesion depth by 43%, compared to control ($p < 0.05$). The cell viability at 7 days against the new cement extracts was 82.2% of that of the negative control in culture medium without any extracts.

Conclusions: The novel orthodontic cement containing $nCaF_2$ and DMAHDM achieved much stronger antibacterial and remineralization capabilities and greater enamel hardness than the commercial control did, without compromising the orthodontic bracket-enamel SBS and biocompatibility.

Clinical Significance: The novel bioactive and nanostructured orthodontic cement is promising to inhibit enamel demineralization, white spot lesions and caries in orthodontic treatments.

1. Introduction

Orthodontic treatments are becoming increasingly popular around the world with patients seeking to improve their esthetics [1]. However, white spot lesions (WSLs) is a major complication in orthodontic therapy and is a barrier to achieving esthetics [2]. WSLs have a chalky appearance around the fixed orthodontic appliances, caused by enamel demineralization due to acids from biofilms in areas adjacent to the brackets and bonding agents [3]. Various interventions attempted to inhibit the enamel demineralization in orthodontic treatments, including the use of fluoride-containing products, chlorhexidine rinses, diet modification, and calcium-containing remineralization products

* Corresponding author.
** Corresponding author.
*** Corresponding author.
E-mail addresses: tuzizhangke@163.com (K. Zhang), zhzhao@scu.edu.cn (Z. Zhao), hxu@umaryland.edu (H.H.K. Xu).

https://doi.org/10.1016/j.jdent.2019.07.010
Received 29 April 2019; Received in revised form 16 July 2019; Accepted 17 July 2019
0300-5712/ Published by Elsevier Ltd.

[4]. However, the prerequisite for their effectiveness is patient compliance, which is often unreliable, especially for children and teenage patients [5]. Therefore, the developments of novel and effective approaches are of critical importance to prevent WSLs.

Fluoride (F) is a dual-functional anti-caries agent, acting on suppressing oral microbes and promoting the remineralization of tooth tissues [6–8]. Fluoride has been used to combat WSLs and caries [9–12]. Resin-modified glass ionomer cements (RMGIs) were used as orthodontic cements with the release of fluoride ions [13,14]. However, the fluoride release from RMGIs decreased rapidly after the initial burst, hence the effect was not sustained [15]. Several clinical trials found that the fluoride concentration released from RMGIs *in vivo* was not high enough to suppress the biofilm metabolism in the long-term [16,17]. Therefore, the development of new orthodontic cements that can release fluoride to the surrounding enamel at a sufficiently high and effective rate is needed to prevent WSLs.

Nanotechnology is promising to improve the performance of various dental materials. The small sizes of nanoparticles and the resultant high surface area enabled a high level of ion release at a relatively low filler level in dental composites [18]. Moreover, nanoparticles were more effective than traditional particles to treat bacterial adherence and oral biofilm formation [19]. Nanomaterials could also optimize the remineralization because the process of caries-induced demineralization started at the nano-level [19]. Therefore, efforts were made to develop nanostructured dental resin materials [20–22]. Calcium fluoride (CaF_2) showed the ability to serve as a labile fluoride reservoir [23]. We previously synthesized calcium fluoride nanoparticles ($nCaF_2$) using a spray-drying technique, achieving high levels of fluoride release without hampering the mechanical properties for dental composite [24–26]. However, to date, there has been no report on the incorporation of $nCaF_2$ into orthodontic cement to combat WSLs.

The low pH around orthodontic brackets due to cariogenic bacteria hinders the remineralization process [27], which should account for the low efficacy of RGMIs to combat WSLs [28]. Incorporating antibacterial monomers into RMGI to inhibit the bacteria is promising to improve its ability to prevent demineralization [29,30]. Quaternary ammonium methacrylates (QAMs) cause bacterial lysis by penetrating bacterial membranes with their alkyl chains [31]. Recently, a new QAM, dimethylaminohexadecyl methacrylate (DMAHDM), was synthesized and exhibited strong anti-biofilm ability when incorporated into dental resins [32]. Nevertheless, there has been no report on the combined incorporation of DMAHDM and $nCaF_2$ into dental resins.

The objectives of the present study were to: (1) develop a new orthodontic cement by incorporating $nCaF_2$ and DMAHDM into RMGI for the first time; and (2) investigate the antibacterial functions, fluoride and calcium ion release, remineralization and enamel hardness properties. It was hypothesized that: (1) the enamel bond strength of RMGI would not be compromised by incorporating $nCaF_2$ and DMAHDM; (2) The RMGI containing $nCaF_2$ could release higher levels of fluoride ions than RMGI control; (3) RMGI containing DMAHDM and $nCaF_2$ would have much stronger antibacterial properties than RMGI control; (4) The incorporation of $nCaF_2$ into RMGI would increase the remineralization ability, resulting in greater enamel hardness than the control orthodontic cement.

2. Materials and methods

2.1. Synthesis of $nCaF_2$

The $nCaF_2$ was synthesized using a spray-drying method [24,25]. Briefly, calcium hydroxide [$Ca(OH)_2$] and ammonium fluoride (NH_4F) were dissolved in distilled water separately to prepare two solutions that provided calcium and fluoride, respectively. The two solutions, at a calcium/fluoride molar ratio of 1:2, were mixed at the time of atomization by a two-liquid nozzle (ViscoMist, Lechler, IL, USA), and sprayed into the heated chamber of the dryer, in which calcium hydroxide and ammonium fluoride reacted together to produce the nano-sized droplets. Subsequently, the droplets were dried in the heated chamber, resulting in the production of nanopowders, which was then collected by an electrostatic precipitator (MistBuster, Air Quality Eng, MN, USA). The reaction of $Ca(OH)_2$ and NH_4F led to the production of CaF_2, NH_3 and H_2O. The NH_3 and H_2O vapors were discharged from the heated chamber with the air flow. The dried nanopowder was collected and was confirmed to be CaF_2 by X-ray diffraction in a previous study [24]. Transmission electron microscopy (TEM, 3010-HREM, JEOL, Peabody, MA, USA) was used to observe and determine the size range and average size of the $nCaF_2$ particles.

2.2. Incorporation of $nCaF_2$ into RMGI

A RMGI (GC Ortho LC, Fuji, Aichi-ken, Japan), referred to as GC, was used as the parental system. GC has been used as a bracket-bonding adhesive in orthodontics due to good bond strength and fluoride-releasing capability. GC consisted of fluoroaluminosilicate glass, hydroxyethyl methacrylate and a light-sensitive, aqueous polyalkenoic acid. The mass ratio of powder to liquid for GC was 2.5:1, according to the manufacturer's instructions. Four mass fractions of $nCaF_2$ were incorporated into GC: 5, 10, 20 and 30%. Mass fractions higher than 30% were not used because of reductions in bonding strength.

2.3. Incorporation of DMAHDM into RMGI

DMAHDM was synthesized through a modified Menschutkin reaction technique [32]. The reaction products from this approach required minimal purification for experimental use [32,33]. Briefly, 10 mmoL of 2-(dimethylamino) docecane (Sigma-Aldrich, St. Louis, MO, USA), 10 mmoL of 1-bromohesadecane (TCI America, Portland, OR, USA) and 3 g of ethanol were mixed and stirred at 70 °C for 24 h. DMADHM was then collected after removing the solvent by evaporation. DMAHDM was added into GC at 4 different mass fractions: 1%, 2%, 3% and 4%. DMAHDM mass fractions greater than 4% were not used to avoid compromising the enamel bond strength.

2.4. Enamel shear bond strength (SBS) testing

Human premolars extracted for orthodontic reasons were collected and stored in 0.1% thymol solution at 4 °C. The use of teeth was approved by the Institutional Review Board of authors' affiliation. Teeth with buccal enamel lesions or other irregularities were excluded. After embedding each premolar vertically into a self-curing acrylic resin (Lang Dental Manufacturing, Wheeling, IL, USA) to guarantee that the buccal surface would be parallel to the force in shear bond strength test, premolar metal orthodontic brackets (Shinye, Hangzhou, China) were bonded to the center of buccal surface. The unmodified GC and another orthodontic cement (Transbond XT, 3 M, Monrovia, CA, USA) were used as controls [28]. According to the manufacturer, the Transbond XT cement consisted of 70–80% silane-treated quartz, 10–20% bisphenol-A-diglycidyl ether dimethacrylate, 5–10% bisphenol-A-bis (2-hydroxyethyl) dimethacrylate, 2% silane-treated silica and about 0.2% diphenyliodonium hexafluorophosphate. The following groups were tested for SBS:

(1) Transbond XT (termed as TB control)
(2) GC control
(3) GC + 5% $nCaF_2$
(4) GC + 10% $nCaF_2$
(5) GC + 20% $nCaF_2$
(6) GC + 30% $nCaF_2$
(7) GC + 1% DMAHDM
(8) GC + 2% DMAHDM
(9) GC + 3% DMAHDM
(10) GC + 4% DMAHDM

(11) GC + 20% $nCaF_2$ + 3% DMAHDM

For each group, the brackets were bonded to the teeth using a standardized method. Briefly, the center of buccal surface was etched with 37% phosphoric acid gel (3 M Unitek, Monrovia, CA, USA) for 30 s, and then dried by an air stream. For groups 1 and 2, the brackets were bonded to the buccal surface following the manufacturers' instructions. For groups 3 to 11, the bonding procedures were the same as that for GC control. A compressive force of 200 g was applied to the bracket for 5 s with a force gauge. Samples were photo-cured (VCL 401, Demetron, CA, USA) at 45° angle and 2 mm away from the enamel surface with 20 s each at the mesial and distal sides, respectively, for a total of 40 s [34].

The SBS test was performed after the bracket-bonded samples were immersed in distilled water at 37 °C for 24 h. A chisel was connected to a computer-controlled universal testing machine (MTS Systems Corporation, Eden prairie, MN, USA), and positioned above the bracket base. The load in the occlusal-gingival direction was applied to the bracket base at a rate of 0.5 mm/min until the bracket was debonded. The SBS was calculated by dividing the load by the bracket contact surface area with enamel [34].

2.5. Specimen fabrication

The SBS test showed that the bonding strength decreased significantly when the mass fractions of $nCaF_2$ and DMAHDM exceeded 20% and 3%, respectively. Therefore, the following five groups were used for the subsequent experiments: TB control; GC control; GC + 20% $nCaF_2$; GC + 3% DMAHDM; GC + 20% $nCaF_2$ + 3% DMAHDM.

2.6. Fluoride (F) and Calcium (Ca) ion release measurement

The pH of a sodium chloride solution (133 mmol/L) was buffered to 4.0, 5.5 and 7.0, by adding lactic acid (50 mmol/L), acetic acid (50 mmol/L) and HEPES (50 mmol/L), respectively. The cement paste was placed into a rectangular mold of 2 × 2 × 12 mm and light-cured for 1 min. Three specimens of each group were immersed in 50 mL of solution at each pH, yielding a ratio of specimen/solution volume to be 2.9 mm^3/mL, following a previous study [24]. The concentrations of F and Ca ions released from cement specimens into solutions at each pH were assessed at 1, 3, 7, 14, 21, 28, 35, 42, 49, and 56 d. For each measurement, 0.5 mL aliquot was collected, and 0.5 mL of fresh solution was added back in. F ion concentration was determined using a selective electrode (Thermo Scientific, Waltham, MA, USA) [24,25]. The concentration of Ca was assessed via a spectrophotometric method (SpectraMax M5, Molecular Devices, Sunnyvale, CA, USA) [21].

2.7. Dental plaque microcosm biofilm formation

Human saliva was employed to establish the microcosm biofilm *in vitro* due to the advantage of maintaining much of the complexity and heterogeneity of dental plaque *in vivo* [35]. Saliva was collected from 10 donors that were required to have natural dentition without caries and no history of antibiotics within the past three months. An equal volume of saliva from each donor were mixed together, and then diluted by sterile glycerol to a concentration of 70% to form the saliva sample [36]. The samples were stored at -80 °C for future use.

Each cement paste was placed into a circular mold with a diameter of 8 mm and a thickness of 1 mm, and light-cured for 1 min. The cement disks were immersed in distilled water and stirred using a magnetic bar at a speed of 100 rpm for 1 h to remove any uncured monomers, following a previous study [37]. Then the disks were sterilized with ethylene oxide (Anprolene AN 74i, Andersen, Haw River, NC, USA) and de-gassed for 7 days.

The McBain artificial saliva medium was prepared [38]. The saliva sample was added into the McBain medium with a volume ratio of 1:50 to prepare the inoculum [36]. A cement disk and 1.5 mL of inoculum were added to each well of 24-well plate and incubated at 37 °C in 5% CO_2 for 8 h. Then, the cement disks were transferred to new 24-well plates and incubated with fresh medium for 16 h. After that, the disks were transferred to new 24-well plates with fresh medium and cultured for another 24 h. The total of 48 -h culture could form relatively mature dental plaque microcosm biofilm on the cements [36].

2.8. Live/dead staining of biofilms

The cement disks with 2-day biofilms were washed with PBS and then stained using a live/dead kit (Molecular Probes, Eugene, OR, USA) following the manufacturer's instruction. The live bacteria were stained with Syto9, and the dead bacteria were stained with propidium iodide, thus producing green and red fluorescence, respectively. The stained disks were examined using an inverted epifluorescence microscope (Eclipse TE2000-S, Nikon, Melville, NY, USA) [28]. Six specimens were prepared for each group, and three fields of view were chosen randomly for each specimen, thus leading to 18 images for each group.

2.9. MTT metabolic assay

The MTT assay was performed to investigate the metabolic activity of biofilms on cement disks. Disks with 2-day biofilms were transferred to a new 24-well plate, immersed by 1 mL of MTT solution (0.5 mg/mL MTT in PBS), and incubated at 37 °C at 5% CO_2 for 1 h. Then the disks were transferred to a new 24-well plate with 1 mL of dimethyl sulfoxide (DMSO), and incubated with gentle mixing for 20 min. Then 200 μL of DMSO solution from each well was transferred to a 96-well plate, and the absorbance at 540 nm (OD_{540}) was assessed using the microplate reader (SpectraMax M5) [28]. Six replicates were texted for each group.

2.10. Biofilm polysaccharide production

The water-insoluble polysaccharide in the extracellular polymeric substance (EPS) was evaluated using a phenol-sulfuric acid method [39]. The cement disks with 2-day biofilms were transferred to tubes containing 2 mL cysteine peptone water (CPW). The biofilms were harvested by sonication and vortexing (Fisher, Pittsburgh, PA, USA). The CPW containing the biofilm was transferred to an Eppendorf tube and centrifuged at 12,000 rpm for 3 min. The precipitate was rinsed with phosphate buffer saline (PBS) and placed in 1 mL of deionized water, which was transferred to a vial with 1 mL of 6% phenol solution and 5 mL of 95% sulfuric acid, and incubated at 37 °C at 5% CO_2. After 30 min, 100 μL of the solution was transferred to a 96-well plate, and the absorbance at OD_{490nm} was evaluated with the microplate reader (SpectraMax M5). The glucose standard solution with concentrations of 0, 5, 10, 20, 50 and 100 mg/L were used to establish the standard curve for converting the OD readings to the polysaccharide concentrations [39]. Six replicates were texted for each group.

2.11. Lactic acid production by biofilms

The lactic acid production of biofilms was measured using an enzymatic method. Cement disks with 2-day biofilms were transferred to new 24-well plates and immersed by 1.5 mL of buffered peptone water containing 0.2% sucrose. The plates were then incubated at 37 °C in 5% CO_2 for 3 h to allow the biofilms to produce lactic acid. After that, the BPW were collected, and the absorbance at 340 nm was measured using a microplate reader (SpectraMax M5). The lactic acid standard solutions were used to prepare the standard curve [28]. Six specimens were used for each group.

2.12. Colony-forming unit (CFU) counts

Cement disks with 2-day biofilms were transferred into tubes

containing 2 mL of CPW, and the biofilms were collected by sonication and vortexing (Fisher). Three types of agar plates were prepared [38]. Tryptic soy blood agar plates were used to determine the total microorganisms. Mitis salivarius agar (MSA) culture plates that contained 15% sucrose were used to assess the viability of all streptococci. MSA agar plates containing 0.2 units of bacitracin/mL was used to evaluate mutans streptococci. The CPW containing the harvested biofilms were serially diluted and then spread onto the three types of agar plates for the CFU analysis [38]. Six replicates were texted for each group.

2.13. Artificial enamel lesions and remineralization

Human third molars were collected from clinics with the approval by the Institutional Review Board of authors' affiliation and with patients' informed consent. After removing the roots and tips, enamel samples of approximate 1 mm thickness were prepared by cutting parallel to the mesial and distal surface using a diamond disk. The samples were embedded in acrylic resin, and then polished with a decreasing sequence of silicon carbide papers (320, 600, 1200 and 2400 grit, Extec, Enfield, CT, USA) with the aid of a water-cooled polishing machine (Handler Manufacturing Co, Westfield, NJ, USA) to ensure that the upper and lower surfaces of each sample were flat and parallel. An enamel surface area of approximate 4 mm × 4 mm was exposed, and the rest of the enamel was covered using an acid-resistant nail varnish.

The remineralization ability of orthodontic cements was investigated. Briefly, cement bars of 2 mm × 2 mm × 12 mm were prepared for the five groups as described in Section 2.5, and the enamel samples were randomly divided to the five groups. Three cement bars were placed on each enamel sample, following previous studies [40–42]. The samples were subjected to 30 days of demineralization-remineralization cycles by immersing in pH-cycling solutions. For each day, samples were immersed in the demineralization solution for 1 h and in the remineralization solution for 23 h. The demineralization solution was prepared by dissolving 3.0 mmol/L $CaCl_2$, 1.8 mmol/L K_2HPO_4, 0.1 mol/L lactic acid and 1% carboxymethylcellulose in deionized water, adjusted to pH 4.0. The 1 -h immersion in demineralization solution approximated the daily accumulated acid challenge times orally [41,43]. The remineralization solution was used to mimic human saliva that could provide Ca and P ions for remineralization. The remineralization solution contained 1.2 mmol/L $CaCl_2$, 0.72 mmol/L K_2HPO_4 and 50 mmol/L HEPES buffer, adjusted to pH 7.0 with KOH (1 mmol/L).

2.14. Surface hardness test and lesion depth analysis

A low hardness in enamel indicated demineralization, while an increased hardness indicated remineralization [44]. The surface hardness of enamel specimens after the 30-day demineralization-remineralization regimen were measured using a hardness tester with a Knoop indenter (Shimadzu Corporation, Kyoto, Japan) under a 25 g load for a dwell time of 5 s. In addition, the hardness value of healthy enamel was also measured as control. Six indentations were made in each enamel sample, and six enamel samples were tested for each group.

The lesion depths were determined following the method in a previous study [40]. After the demineralization-remineralization cycles, the specimens were longitudinally sectioned in the middle of the enamel. Cross-sectional hardness testing was performed using a Knoop indenter (Shimadzu Corporation) under a 25 g load for a dwell time of 5 s. The hardness test was conducted with 30 indentations distributed in three rows of 10 indentations each. The three rows were located at the three quartiles of the demineralized enamel, with an interval of 1 mm between each other. In each row, every indentation was spaced 20 μm away from the neighboring indentations. The hardness profile was obtained by plotting the hardness values versus enamel depths. The hardness profile of sound enamel was evaluated as the control. The lesion depth was determined by using the depth where the enamel hardness reached that of the sound enamel [40]. For each specimen, the lesion depth was determined as the average value of the lesion depths in the three rows.

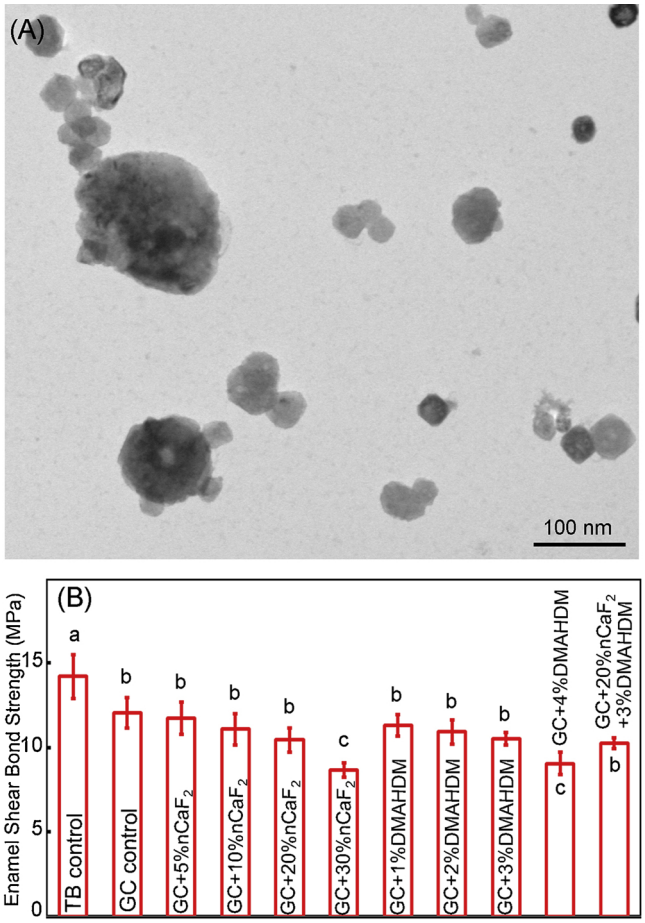

Fig. 1. CaF_2 nanoparticles and enamel shear bond strengths. (A) Typical TEM image of CaF_2 nanoparticles ($nCaF_2$). (B) Enamel shear bond strengths of modified RMGI (mean ± sd; n = 6). The incorporation of $nCaF_2$ and DMAHDM did not adversely affect the bond strength ($p > 0.1$), until the mass fraction reached 30% and 4%, respectively. Adding 20% $nCaF_2$ and 3% DMAHDM did not cause a significant difference ($p > 0.1$). The same letters in (B) indicate no statistical difference between the groups ($p > 0.1$), while the different letters in (B) indicate a significant difference ($p < 0.05$).

2.15. Cytotoxicity analysis

Human gingival fibroblasts (HGF, ScienCell, San Diego, CA, USA) was cultured in Dulbecco's Modified Eagle Medium (DMEM) with 10% fetal calf serum (FCS), 100 IU/mL penicillin and 100 IU/mL streptomycin. Six cement disks, 1 mm thick and 8 mm in diameter, were prepared for each group. The cement disks went through 1 -h stir in distilled water to remove the initial burst of uncured monomers, and were then sterilized with ethylene oxide (Anprolene AN 74i) as described in Section 2.7. Then each disk was immersed by 500 μL of cell culture medium (without FCS) in a 48-well plate, yielding the ratio of cement surface area to solution volume to be approximately 2.5 cm^2/mL, which is within the 0.5-6.0 cm^2/mL range recommended by the ISO [45,46]. The disks were incubated at 37°C in dark. The cell culture medium was replaced daily. The extracts in day 1, 4, and 7 were collected and stored at -20°C for cytotoxicity experiments.

To test the cytotoxicity, the HGFs (passage 8) were seeded into 96-well plates with a cell density of approximately 10,000 cells for each

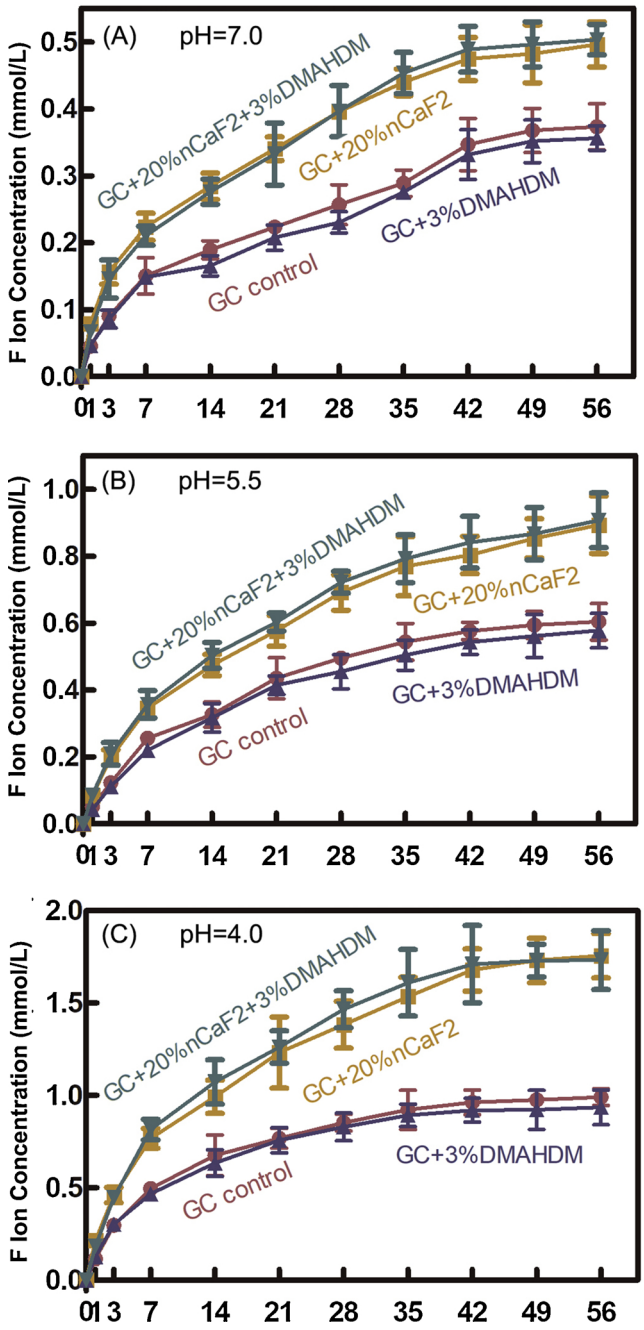

Fig. 2. Fluoride (F) ion release from orthodontic cements (mean ± sd; n = 6) at pH 7.0 (A), pH 5.5 (B), and pH 4.0 (C). Both the incorporation of nCaF and the reduction of pH increased the release of F ions ($p < 0.05$).

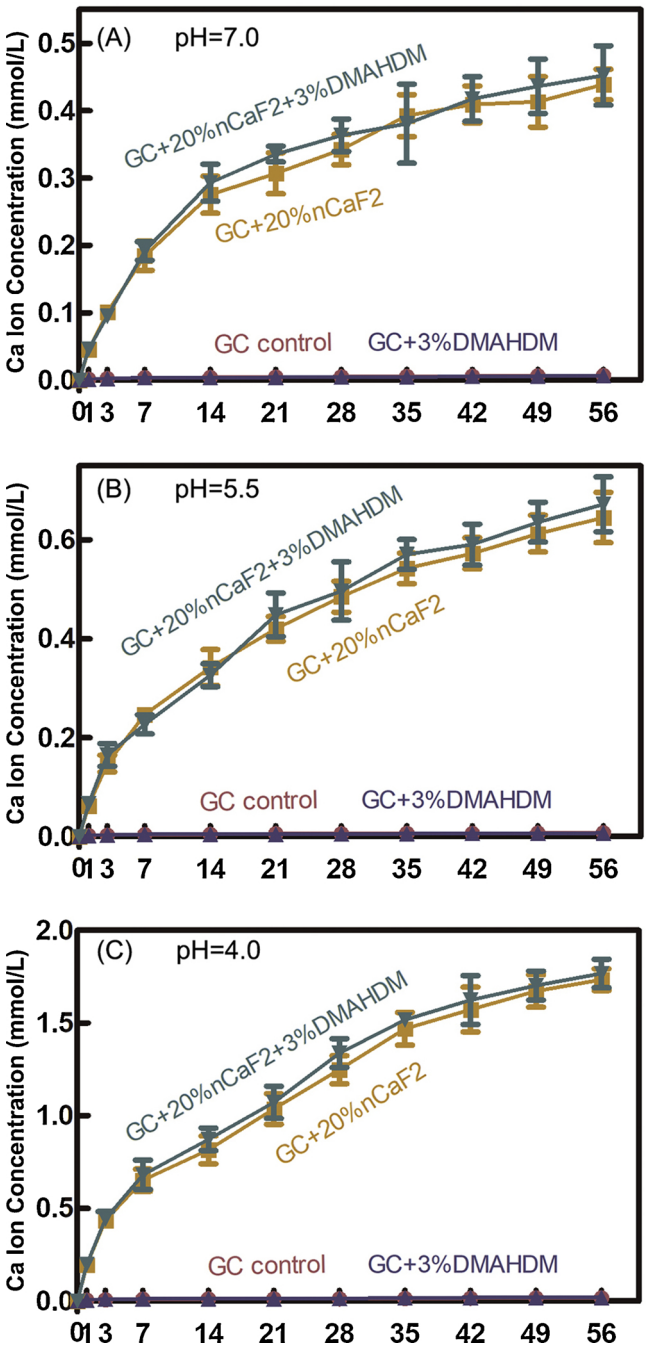

Fig. 3. Calcium (Ca) ion release from orthodontic cements (mean ± sd; n = 6) at pH 7.0 (A), pH 5.5 (B), and pH 4.0 (C). Both the incorporation of $nCaF_2$ and the reduction of pH increased the release of Ca ions ($p < 0.05$).

well. The cells were cultured using 90 µL of extracts plus 10 µL of FCS per well at 37 °C for 24 h. The HGFs in culture medium without any extracts served as control. After 24 -h incubation, 20 µL of MTT solution (5 mg/mL) was added into each well. After 4 -h incubation at 37 °C in the dark, 150 µL of DMSO was added. The optical densities (OD) were measured at 492 nm (SpectraMax M5). The OD ratios of the experimental groups to that of the control group were plotted as the cell viability [47].

2.16. Statistical analysis

SPSS (version 19.0, SPSS Inc, Chicago, IL, USA) was used. All data were expressed as means ± standard deviations. The normal distribution of all data was identified by Shapiro-Wilk Analysis. The specimen size for each group was determined as n = 6 based on the typical standard deviation of around 20% of the mean value and at least 100% difference between groups in our pilot study. One-way and two-way analyses of variance were performed, followed by Fisher's Least Significant Difference post-hoc test. Differences with $p < 0.05$ were considered as being statistically significant.

3. Results

A representative TEM image of the $nCaF_2$ is shown in Fig. 1A. The $nCaF_2$ consisted a combination of fine nanoparticles and relatively larger nanoparticles. The fine nanoparticles had a size of approximately10 nm, while the larger nanoparticles had sizes of about

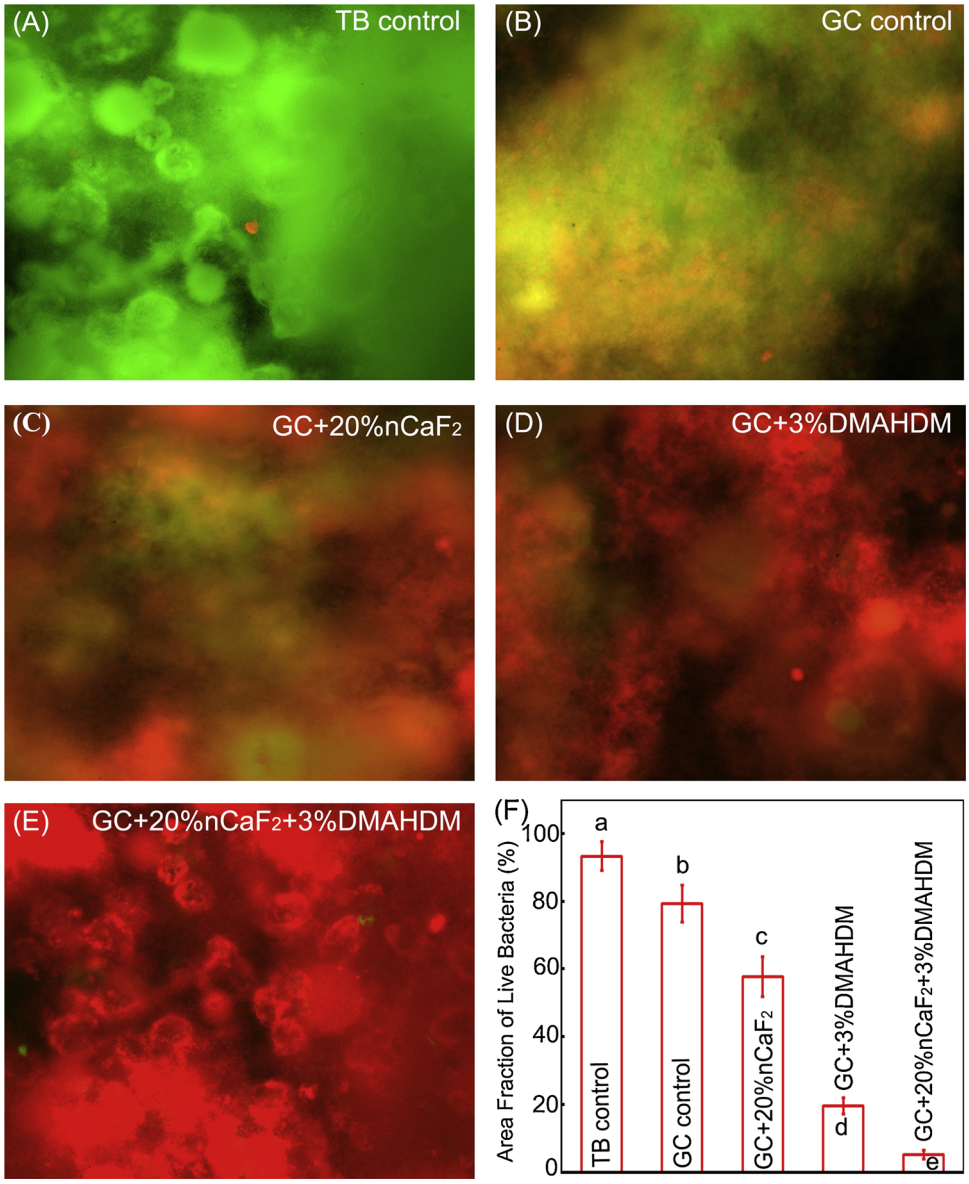

Fig. 4. Representative live/dead staining images of biofilms grown on resin disks: (A) TB control, (B), GC control, (C) $nCaF_2$ group, (D), DMAHDM group, and (E) $nCaF_2$ + DMAHDM group. (F) Area fraction of live bacteria on resin disks (mean ± sd; n = 6). Live bacteria were stained green. Dean bacteria were stained red. Yellow and orange indicated that live and dead bacteria were in close proximity or on the top/bottom of each other. The different letters in (F) indicate significant differences ($p < 0.05$) (For interpretation of the references to colour in this figure legend, the reader is referred to the web version of this article).

100–200 nm. The larger nanoparticles appeared to be formed by the fusion of numerous fine nanoparticles, which likely took place in the spray-drying chamber before the wet particles were fully dried. The sizes of 100 randomly-selected nanoparticles were measured via TEM. The $nCaF_2$ particle size ranged from approximately 15 nm to 247 nm, with (mean ± SD; n = 100) of (58 ± 43) nm.

The enamel SBS results are shown in Fig. 1B. TB control had the highest SBS ($p < 0.05$). Increasing the mass fraction of $nCaF_2$ from 0% to 20% had no negative effect on SBS ($p > 0.1$). However, a further increment to 30% caused a significant decrease in SBS, compared to GC control ($p < 0.05$). Similarly, the SBS of GC was not compromised until the mass fraction of DMAHDM reached 4% ($p < 0.05$). The 20% $nCaF_2$ + 3% DMAHDM group had similar SBS to GC control ($p > 0.1$).

The F ion releases at pH 7.0, 5.5 and 4.0 are plotted in Fig. 2. Both the incorporation of $nCaF_2$ and pH values had significant effects on the release of F ions. The amount of released F ions was significantly enhanced by incorporating $nCaF_2$ ($p < 0.05$), while the incorporation of DMAHDM did not decrease the F release ($p > 0.1$). The reduction in pH values also promoted the release of F ions ($p < 0.05$).

The Ca ion releases are shown in Fig. 3. The concentrations of Ca ions were similar between the two groups containing $nCaF_2$ ($p > 0.1$), and significantly higher than GC control group and GC + 3% DMAHDM group, which were nearly zero ($p < 0.05$). Similar to the F ions, decreasing the pH to 5.5 greatly improved the Ca ion release compared to the pH of 7.0 ($p < 0.05$), which was further facilitated by bringing pH down to 4.0 ($p < 0.05$).

Representative live/dead images of 2-day biofilms on cements are displayed in Fig. 4. TB control was fully covered by live biofilm. GC control had primarily live bacteria, with a few spots of dead bacteria ($p < 0.05$). The amount of dead bacteria increased in GC + 20% $nCaF_2$ group ($p < 0.05$), and was further increased in GC + 3% DMAHDM group ($p < 0.05$). GC + 20% $nCaF_2$ + 3% DMAHDM was covered by mostly dead bacteria with few live bacteria ($p < 0.05$).

The metabolic activity of biofilms is plotted in Fig. 5A. The metabolic activity of biofilms on TB control was the highest, followed by GC control ($p < 0.05$). The incorporation of $nCaF_2$ or DMAHDM alone

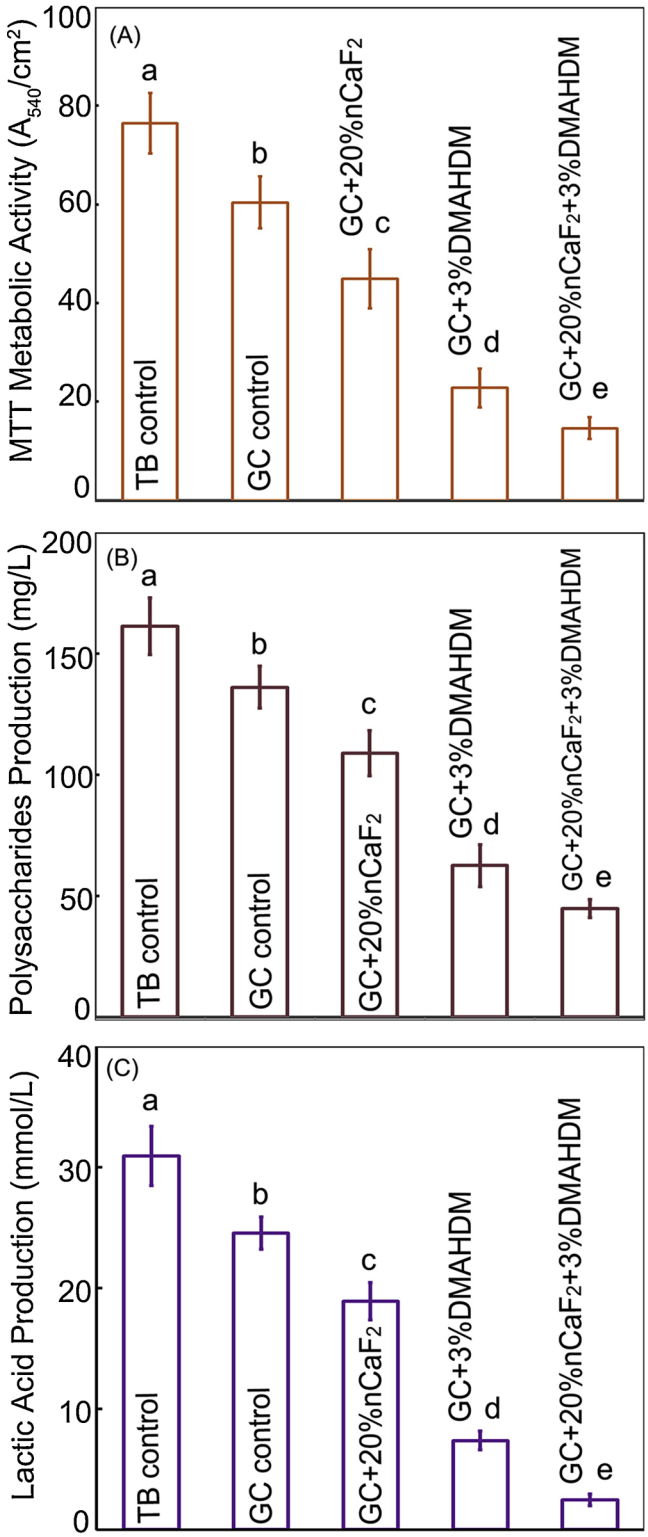

Fig. 5. Quantitative antibacterial effects for biofilms grown on cements (mean ± sd; n = 6): (A) MTT assay, (B) lactic acid production, (C) polysaccharide production. The incorporation of $nCaF_2$ and DMAHDM reduced the metabolic activity, lactic acid production, and polysaccharide ($p < 0.05$). In each plot, different letters indicate significant differences between groups ($p < 0.05$).

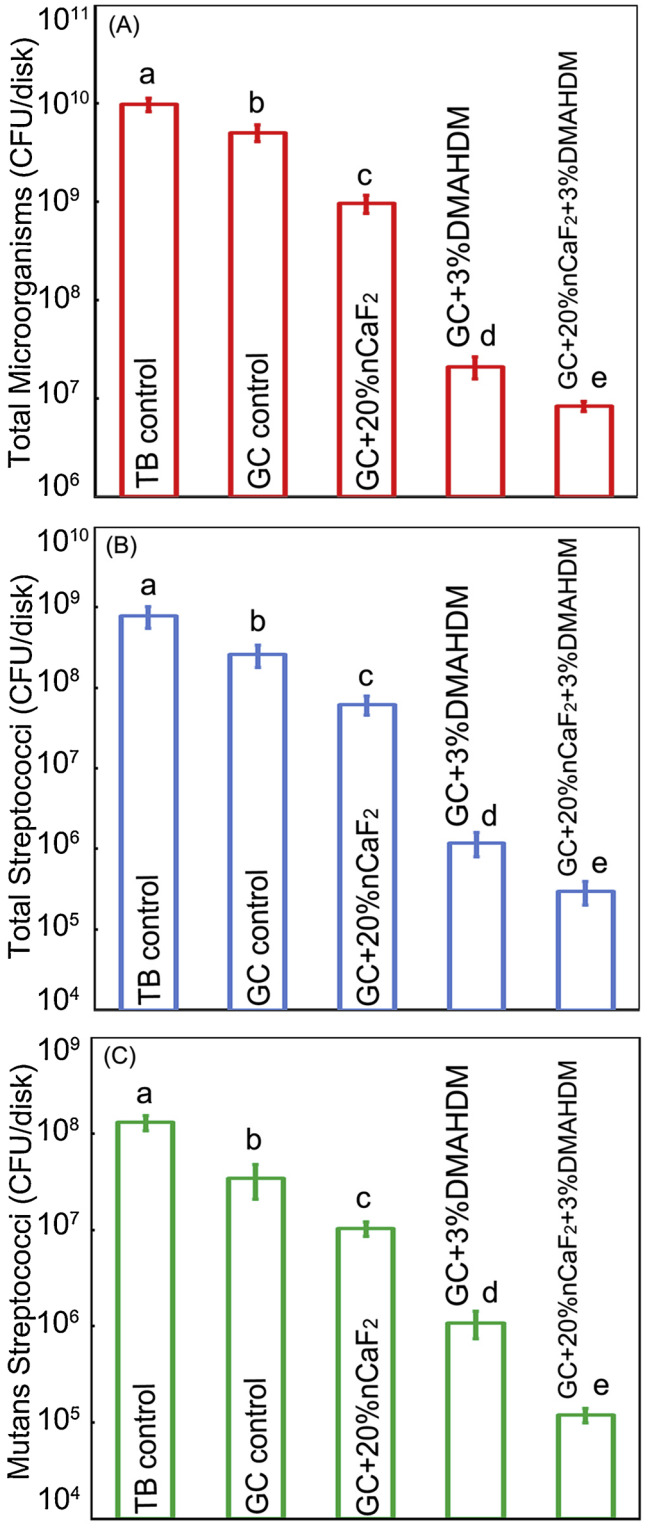

Fig. 6. Colony-forming unit (CFU) counts of 2-day biofilms on cement disks (mean ± sd; n = 6): (A) total microorganisms, (B) total streptococci, and (C) mutans streptococci. The incorporation of $nCaF_2$ and DMAHDM reduced all three CFU counts by more than three orders of magnitude ($p < 0.05$). In each plot, different letters indicate significant differences between groups ($p < 0.05$).

significantly decreased the metabolic activity of biofilms ($p < 0.05$). The incorporation of $nCaF_2$ and DMAHDM simultaneously resulted in the least metabolic activity, which was only 19.1% and 24.2% of that in the TB control and GC control group respectively ($p < 0.05$).

Fig. 5B plots the polysaccharide production of biofilms. The polysaccharide production of GC control was lower than TB control ($p < 0.05$), but higher than the GC + 20% $nCaF_2$ group and GC + 3%

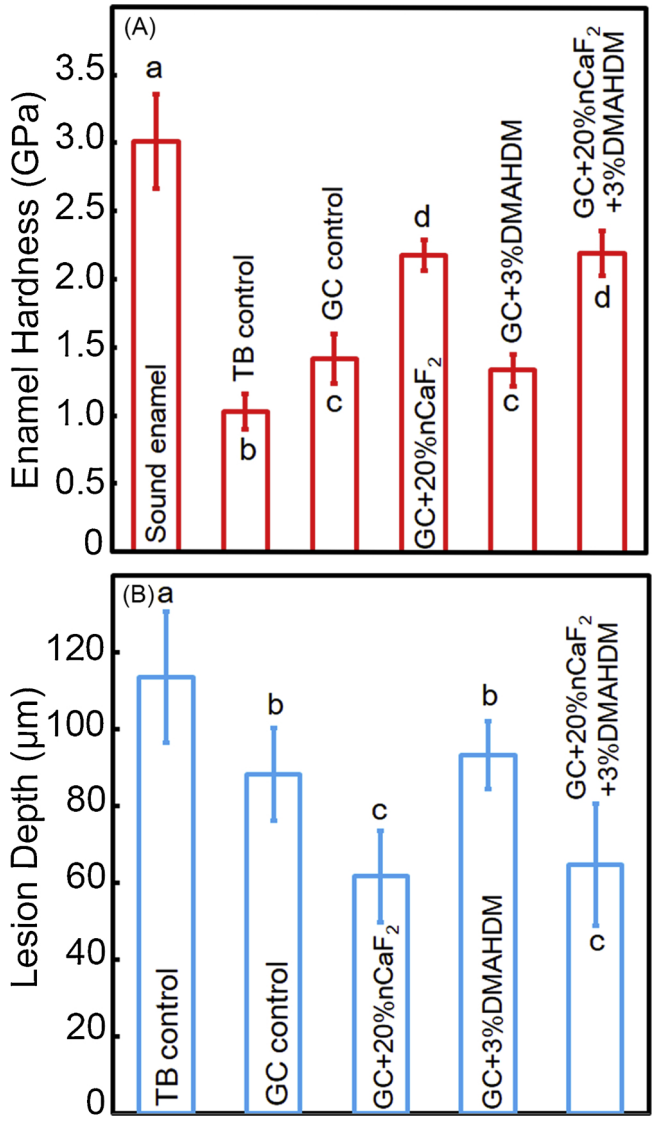

Fig. 7. Remineralization of enamel after 30 days of demineralization-remineralization cycles (mean ± sd; n = 6). (A) Surface hardness of enamel. (B) Lesion depth of enamel. The incorporation of $nCaF_2$ greatly improved the enamel hardness and decreased the lesion depth, when compared to commercial control ($p < 0.05$). In each plot, the different letters indicate significant differences between groups ($p < 0.05$).

DMAHDM group ($p < 0.05$). The polysaccharide production was least on GC + 20% $nCaF_2$ + 3% DMAHDM, which was 27.7% and 32.8% of that in the TB control and GC control group respectively ($p < 0.05$).

The lactic acid production of biofilms on cements is presented in Fig. 5C. Biofilms on TB produced the most acid, followed by GC control ($p < 0.05$). The $nCaF_2$-containing or DMAHDM-containing cements produced less lactic acid than GC control ($p < 0.05$). Biofilms on GC containing both $nCaF_2$ and DMAHDM had the least acid, which was 7.9% and 9.7% of that in the TB control and GC control group respectively ($p < 0.05$).

The CFU counts of 2-day biofilms grown on cement disks are shown in Fig. 6: (A) Total microorganisms, (B) total streptococci and (C) mutans streptococci. TB control had the highest CFU, followed by GC control ($p < 0.05$). The incorporation of $nCaF_2$ caused a significant reduction in biofilm CFU ($p < 0.05$). The incorporation of DMAHDM decreased the CFU by nearly 3 orders of magnitude ($p < 0.05$). The incorporation of $nCaF_2$ and DMAHDM resulted in the least CFU, which was more than 3 orders of magnitude less than that on GC control ($p < 0.05$).

The surface hardness of enamel specimens are shown in Fig. 7A. After the 30-day demineralization-remineralization cycles, the enamel hardness of TB control group was significantly decreased, compared to sound enamel ($p < 0.05$). In contrast, GC control and GC + 3% DMAHDM group yielded greater enamel hardness than TB control ($p < 0.05$). The two groups containing $nCaF_2$ had even greater enamel hardness ($p < 0.05$).

The lesion depths of enamel specimens are plotted in Fig. 7B. The TB control had the highest lesion depth ($p < 0.05$), followed by GC control and GC + 3% DMAHDM group. GC + 20% $nCaF_2$ group and GC + 20% $nCaF_2$ + 3% DMAHDM group had the lowest lesion depths ($p < 0.05$).

The viability of HGFs cultured with extracts of the cements is plotted in Fig. 8. Culturing HGFs with the extracts of cements resulted in different cell viability values. The extracts of TB control had the highest cell viability at all three time points ($p < 0.05$). For the extracts of day 1 and 4, GC control and GC + 3% DMAHDM had similar cell viability ($p > 0.1$). For the extracts of day 7, no significant differences were observed between the two groups with $nCaF_2$ and the two without $nCaF_2$ ($p > 0.1$).

4. Discussion

In the present study, we developed a novel orthodontic cement by incorporating $nCaF_2$ and DMAHDM into a RMGI for antibacterial and remineralization capabilities. The hypotheses were proven that incorporating $nCaF_2$ and DMAHDM at appropriate mass fractions did not decrease the enamel bond strength; the F release was greatly increased with the addition of $nCaF_2$; RGMI containing $nCaF_2$ and DMAHDM inhibited biofilm growth and acid production; and the remineralization capability of RMGI and enamel hardness were significantly increased by the new orthodontic cement.

A key requirement for orthodontic cements is sufficient enamel bond strength. The minimum of clinically-acceptable SBS for metal brackets was 7.8 MPa [48], and the SBS of commercial orthodontic adhesives ranged from 10.1 MPa to 19.0 MPa [49], which were high enough to avoid the accidental debonding during lengthy treatments, but not too high to damage the enamel during the removal of brackets when the treatment was finished [49]. In the present study, the SBS was 10.25 MPa for the RMGI containing 20% $nCaF_2$ and 3% DMAHDM, which was within the range of commercial orthodontic cements and higher than the minimum of 7.8 MPa [48,49]. It should be noted that, although previous studies demonstrated that adding bioactive agents into orthodontic adhesives could decrease the bond strength [50], the present study identified the appropriate mass fractions of $nCaF_2$ and/or DMAHDM that maintained the bond strength of RMGI to be within the acceptable range.

The present study synthesized $nCaF_2$ via a spray-drying technique, yielding a median particle size of approximately 58 nm. This resulted in a high surface area and enabled a small amount of $nCaF_2$ to release high levels of F ions [51]. This avoided compromising the mechanical properties by having to use high mass fractions of CaF_2 in order to have sufficient F ion release. We previously identified that combining 20% $nCaF_2$ with non-fluoride glass particles in a resin yielded a nanocomposite with F ion release comparable to that of a RMGI [16]. In the present study, incorporating $nCaF_2$ increased the F release during the 8-week period by up to 49%, compared to the unmodified RMGI. Furthermore, the nCaF2-containing RMGI was smart and substantially increased the release of F ions at lower pH, when these ions would be most needed to protect enamel and inhibit demineralization. The placement of fixed orthodontic appliances impedes the oral hygiene maintenance, which could reduce the pH around brackets to below 4.5 [52]. Such a low pH is cariogenic and can cause enamel demineralization, leading to WSLs [53]. Therefore, the smart F release by the new $nCaF_2$-containing orthodontic cement at low pH could help combat

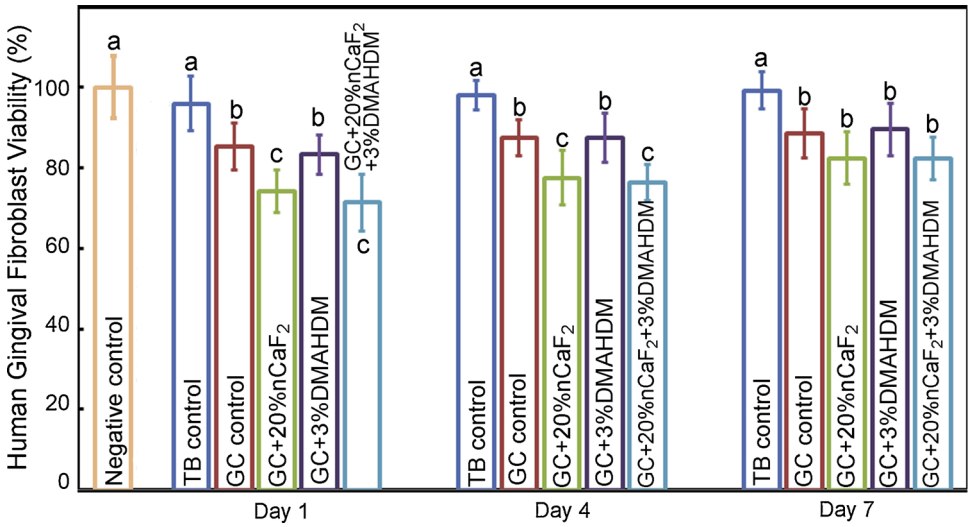

Fig. 8. Cell viability of human gingival fibroblasts after incubation with the orthodontic cement extracts. TB control resulted in the highest cell viability for all three times ($p < 0.05$). For the extracts of day 1 and 4, the two groups containing $nCaF_2$ had lower cell viabilities than those two without $nCaF_2$ ($p < 0.05$). For the extracts of day 7, no difference was detected among them ($p > 0.1$).

WSLs.

Furthermore, the antibacterial capability of RMGI was enhanced by $nCaF_2$, and was further substantially enhanced by the combined use of $nCaF_2$ and DMAHDM. DMAHDM has a wide antimicrobial spectrum and potent antibacterial effects via the contact-inhibition mechanism [54]. DMAHDM is copolymerized with resin by forming covalent bonds with the polymer network, thus is immobilized and is not released or lost over time [54,55]. Therefore, the antibacterial capability of DMAHDM is permanent. However, the antibacterial capability is also limited to biofilm contacting its surface only [54], as biofilms away from DMAHDM cannot be inhibited due to a lack of contact. However, the released F ions could act as the glycolytic enzyme inhibitor and transmembrane proton carrier, thereby inhibiting oral microbes by inducing cytoplasmic acidification, thus possessing a long-distance antibacterial function [6,56]. Therefore, the incorporation of $nCaF_2$ and DMAHDM together possessed antibacterial activity not only against biofilms on the surface, but also against those nearby biofilms away from the surface. This feature would be highly beneficial to prevent WSLs in orthodontic treatments, because the dental plaque in the vicinity of the brackets could also produce organic acids to induce enamel demineralization [57,58].

Another promising approach to inhibit WSLs is to promote the remineralization of decalcified enamel. The low-pH microenvironment produced by bacteria could preferentially react with the phosphate group of the hydroxyapatite in enamel, leading to enamel dissolution [59,60]. However, F ions could enhance remineralization by forming fluoroapatite [$Ca_5(PO_4)_3F$] [61]. The chemical nature of fluoride-induced remineralization is through the equilibrium shift to fluoroapatite due to the supersaturated levels of the ions [62]. In the present study, the incorporation of $nCaF_2$ in GC resulted in a much greater enamel hardness and less lesion depth than the control, indicating an effective remineralization capability. The greater enamel hardness and less lesion depth were likely due to three main reasons. First, the increased levels of F ion release from the $nCaF_2$-containing RMGI contributed to the remineralization. Second, the formation of each fluoroapatite unit consumes only one F ion but five Ca ions; therefore, the Ca ions released by $nCaF_2$ also significantly contributed in promoting the remineralization process, yielding a greater enamel hardness. Third, the $nCaF_2$-containing RMGI could induce the formation of fluoroapatite, which was more resistant to the low-pH environment than the normal hydroxyapatite [59]. Therefore, once fluoroapatite was formed, the enamel surface became more stable and protected the underlying enamel from further demineralization during the 30 days of demineralization/remineralization regimen, yielding a greater enamel hardness and lower lesion depth [59].

Regarding potential clinical applications, a requirement for orthodontic cement is biocompatibility. According to the International Standard Organization (ISO) classification, the materials that result in a cell viability below 70% of the negative control should be considered as cytotoxic [46]. In the present study, the RMGI incorporated with $nCaF_2$ + DMAHDM had cell viability values of 71.3%, 76.4% and 82.2% at day 1, 4, and 7, respectively, of the negative control (culture medium without any extracts). These results indicate that the novel cement had an acceptable biocompatibility. The incorporation of $nCaF_2$ into RMGI caused a significant decrease in cell viability at day 1 and 4, but not at day 7, which might be due to the reduction of F ion release with increasing time. It should be noted that the cytotoxicity test of the present study without a constant salivary flow represented a more severe condition than that in the oral environment. Therefore, the difference in cell viability between the new cement and GC control may be eliminated faster when applied in the oral environment with food, drinks and salivary flow. Furthermore, the minor short-term cytotoxicity induced by RMGI is mainly attributed to the unpolymerized monomers including hydroxyethyl methacrylate (HEMA) rather than F ions [63]. Indeed, a previous study showed that the concentrations of inorganic ions released by RMGI were too low to have any cytotoxic effect [64]. A previous study reported that the incorporation of DMAHDM into a composite did not compromise its biocompatibility [47]. This is consistent with the present study showing that the addition of DMAHDM did not cause a significant cytotoxicity. Therefore, the incorporation of $nCaF_2$ and DMAHDM into RMGI had an acceptable biocompatibility. Further studies are needed to investigate cytotoxicity using a flow system and to evaluate biocompatibility *in vivo* using an animal model [46]. Further studies are also needed to investigate the effects of DMAHDM + $nCaF_2$ + RMGI on enamel demineralization, remineralization and hardness in orthodontic applications using tests that simulate the oral conditions *in vivo*.

5. Conclusion

A novel orthodontic cement with antibacterial and remineralization properties was developed by incorporating 20% $nCaF_2$ and 3% DMAHDM into a RMGI, demonstrating the potential to inhibit WSLs with substantial increases in enamel hardness for the first time. The F release of the new cement was greatly increased via $nCaF_2$ addition. The cement was smart and markedly increased the F release at cariogenic pH when these ions would be most needed to combat WSLs. The new cement inhibited biofilm acid and polysaccharide production, and reduced biofilm CFU by 3 log. Due to remineralization by the new cement, the enamel hardness was more than 2-fold, and the lesion depth

was 50% lower than, those of Transbond control group. In addition, the new cement had enamel bond strength comparable to commercial RMGI. Hence, the use of $nCaF_2$ with small particle sizes and high surface area substantially increased the F release to enhance the remineralization efficacy. The combined use of $nCaF_2$ + DMAHDM is promising for applications in other dental cements, sealants, composites and bonding agents to inhibit biofilm acids and promote remineralization.

Declaration of Competing Interest

The authors declare no conflict of interest

Acknowledgement

We thank Dr. Lawrence C. Chow, Dr. Maria Ibrahim, Dr. Abdulrahman Balhaddad and Dr. Bashayer Baras for their assistance. This work was supported by National Natural Science Foundation of China81801018 (JY) and 81400540 (KZ), University of Maryland School of Dentistry bridging fund (HX), and University of Maryland seed grant (HX)

References

[1] P.R. Dos Santos, M.C. Meneghim, G.M. Ambrosano, M.V. Filho, S.A. Vedovello, Influence of quality of life, self-perception, and self-esteem on orthodontic treatment need, Am. J. Orthod. Dentofacial Orthop. 151 (2017) 143–147.
[2] K.C. Julien, P.H. Buschang, P.M. Campbell, Prevalence of white spot lesion formation during orthodontic treatment, Angle Orthod. 83 (2013) 641–647.
[3] S. Lovrov, K. Hertrich, U. Hirschfelder, Enamel demineralization during fixed orthodontic treatment - incidence and correlation to various oral-hygiene parameters, J. Orofac. Orthop. 68 (2007) 353–363.
[4] D. Hochli, M. Hersberger-Zurfluh, S.N. Papageorgiou, T. Eliades, Interventions for orthodontically induced white spot lesions: a systematic review and meta-analysis, Eur. J. Orthod. 39 (2017) 122–133.
[5] G.C. Heymann, D. Grauer, A contemporary review of white spot lesions in orthodontics, J. Esthet. Restor. Dent. 25 (2013) 85–95.
[6] X. Zheng, X. Cheng, L. Wang, W. Qiu, S. Wang, Y. Zhou, M. Li, Y. Li, L. Cheng, J. Li, X. Zhou, X. Xu, Combinatorial effects of arginine and fluoride on oral bacteria, J. Dent. Res. 94 (2015) 344–353.
[7] H. Koo, Strategies to enhance the biological effects of fluoride on dental biofilms, Adv. Dent. Res. 20 (2008) 17–21.
[8] J.M. ten Cate, The need for antibacterial approaches to improve caries control, Adv. Dent. Res. 21 (2009) 8–12.
[9] M.S. Shinohara, M.F. De Goes, L.F. Schneider, J.L. Ferracane, P.N. Pereira, V. Di Hipolito, T. Nikaido, Fluoride-containing adhesive: durability on dentin bonding, Dent. Mater. 25 (2009) 1383–1391.
[10] H.B. Davis, F. Gwinner, J.C. Mitchell, J.L. Ferracane, Ion release from, and fluoride recharge of a composite with a fluoride-containing bioactive glass, Dent. Mater. 30 (2014) 1187–1194.
[11] A. Itthagarun, N.M. King, J.S. Wefel, F.R. Tay, D.H. Pashley, The effect of fluoridated and non-fluoridated rewetting agents on in vitro recurrent caries, J. Dent. 29 (2001) 255–273.
[12] S. Imazato, Antibacterial properties of resin composites and dentin bonding systems, Dent. Mater. 19 (2003) 449–457.
[13] C.D. Lynch, Summary of: a retrospective, practice-based,clinical evaluation of Fuji IX restorations aged over five years placed in load-bearing cavities, Br. Dent. J. 215 (2013) 290–291.
[14] T. Herion, J.L. Ferracane, D.A. Covell Jr., Three cements used for orthodontic banding of porcelain molars, Angle Orthod. 77 (2007) 94–99.
[15] E. Chatzistavrou, T. Eliades, S. Zinelis, A.E. Athanasiou, G. Eliades, Fluoride release from an orthodontic glass ionomer adhesive in vitro and enamel fluoride uptake in vivo, Am. J. Orthod. Dentofacial Orthop. 137 (2010) 458 e451-458; discussion 458-459.
[16] J.W. van Dijken, S. Kalfas, V. Litra, A. Oliveby, Fluoride and mutans streptococci levels in plaque on aged restorations of resin-modified glass ionomer cement, compomer and resin composite, Caries Res. 31 (1997) 379–383.
[17] P.E. Benson, J. Alexander-Abt, S. Cotter, F.M.V. Dyer, F. Fenesha, A. Patel, C. Campbell, N. Crowley, D.T. Millett, Resin-modified glass ionomer cement vs composite for orthodontic bonding: a multicenter, single-blind, randomized controlled trial, Am. J. Orthod. Dentofacial Orthop. 155 (2019) 10–18.
[18] M.D. Weir, J. Ruan, N. Zhang, L.C. Chow, K. Zhang, X. Chang, Y. Bai, H.H.K. Xu, Effect of calcium phosphate nanocomposite on in vitro remineralization of human dentin lesions, Dent. Mater. 33 (2017) 1033–1044.
[19] M. Hannig, C. Hannig, Nanomaterials in preventive dentistry, Nat. Nanotechnol. 5 (2010) 565–569.
[20] J.L. Moreau, M.D. Weir, A.A. Giuseppetti, L.C. Chow, J.M. Antonucci, H.H. Xu, Long-term mechanical durability of dental nanocomposites containing amorphous calcium phosphate nanoparticles, J Biomed Mater Res B Appl Biomater 100 (2012) 1264–1273.
[21] H.H. Xu, J.L. Moreau, L. Sun, L.C. Chow, Nanocomposite containing amorphous calcium phosphate nanoparticles for caries inhibition, Dent. Mater. 27 (2011) 762–769.
[22] C. Chen, M.D. Weir, L. Cheng, N.J. Lin, S. Lin-Gibson, L.C. Chow, X. Zhou, H.H. Xu, Antibacterial activity and ion release of bonding agent containing amorphous calcium phosphate nanoparticles, Dent. Mater. 30 (2014) 891–901.
[23] M. Hannig, C. Hannig, Nanobiomaterials in preventive dentistry, in: K. Subramani, W. Ahmed, J. Hartsfield (Eds.), Nanobiomaterials in Clinical Dentistry, Elsevier Inc, Oxford, UK, 2013, pp. 167–187.
[24] H.H. Xu, J.L. Moreau, L. Sun, L.C. Chow, Strength and fluoride release characteristics of a calcium fluoride based dental nanocomposite, Biomaterials 29 (2008) 4261–4267.
[25] H.H. Xu, J.L. Moreau, L. Sun, L.C. Chow, Novel CaF(2) nanocomposite with high strength and fluoride ion release, J. Dent. Res. 89 (2010) 739–745.
[26] L. Cheng, M.D. Weir, H.H. Xu, A.M. Kraigsley, N.J. Lin, S. Lin-Gibson, X. Zhou, Antibacterial and physical properties of calcium-phosphate and calcium-fluoride nanocomposites with chlorhexidine, Dent. Mater. 28 (2012) 573–583.
[27] H. Badawi, R.D. Evans, M. Wilson, D. Ready, J.H. Noar, J. Pratten, The effect of orthodontic bonding materials on dental plaque accumulation and composition in vitro, Biomaterials 24 (2003) 3345–3350.
[28] N. Zhang, M.D. Weir, C. Chen, M.A. Melo, Y. Bai, H.H. Xu, Orthodontic cement with protein-repellent and antibacterial properties and the release of calcium and phosphate ions, J. Dent. 50 (2016) 51–59.
[29] S. Imazato, Y. Kinomoto, H. Tarumi, S. Ebisu, F.R. Tay, Antibacterial activity and bonding characteristics of an adhesive resin containing antibacterial monomer MDPB, Dent. Mater. 19 (2003) 313–319.
[30] Y. Takahashi, S. Imazato, A.V. Kaneshiro, S. Ebisu, J.E. Frencken, F.R. Tay, Antibacterial effects and physical properties of glass-ionomer cements containing chlorhexidine for the ART approach, Dent. Mater. 22 (2006) 647–652.
[31] S. Imazato, Bio-active restorative materials with antibacterial effects: new dimension of innovation in restorative dentistry, Dent. Mater. J. 28 (2009) 11–19.
[32] H. Zhou, F. Li, M.D. Weir, H.H. Xu, Dental plaque microcosm response to bonding agents containing quaternary ammonium methacrylates with different chain lengths and charge densities, J. Dent. 41 (2013) 1122–1131.
[33] C. Zhou, M.D. Weir, K. Zhang, D. Deng, L. Cheng, H.H. Xu, Synthesis of new antibacterial quaternary ammonium monomer for incorporation into CaP nanocomposite, Dent. Mater. 29 (2013) 859–870.
[34] H.Y. Cheng, C.H. Chen, C.L. Li, H.H. Tsai, T.H. Chou, W.N. Wang, Bond strength of orthodontic light-cured resin-modified glass ionomer cement, Eur. J. Orthod. 33 (2011) 180–184.
[35] A.J. McBain, Chapter 4: In vitro biofilm models: an overview, Adv. Appl. Microbiol. 69 (2009) 99–132.
[36] L. Cheng, R.A. Exterkate, X. Zhou, J. Li, J.M. ten Cate, Effect of Galla chinensis on growth and metabolism of microcosm biofilms, Caries Res. 45 (2011) 87–92.
[37] S. Imazato, A. Ehara, M. Torii, S. Ebisu, Antibacterial activity of dentine primer containing MDPB after curing, J. Dent. 26 (1998) 267–271.
[38] A.J. McBain, C. Sissons, R.G. Ledder, P.K. Sreenivasan, W. De Vizio, P. Gilbert, Development and characterization of a simple perfused oral microcosm, J. Appl. Microbiol. 98 (2005) 624–634.
[39] S. Xiao, H. Wang, K. Liang, F. Tay, M.D. Weir, M.A.S. Melo, L. Wang, Y. Wu, T.W. Oates, Y. Ding, H.H.K. Xu, Novel multifunctional nanocomposite for root caries restorations to inhibit periodontitis-related pathogens, J. Dent. 81 (2019) 17–26.
[40] M.A.S. Melo, M.D. Weir, V.F. Passos, M. Powers, H.H.K. Xu, Ph-activated nano-amorphous calcium phosphate-based cement to reduce dental enamel demineralization, Artif. Cells Nanomed. Biotechnol. 45 (2017) 1778–1785.
[41] S.E. Langhorst, J.N. O'Donnell, D. Skrtic, In vitro remineralization of enamel by polymeric amorphous calcium phosphate composite: quantitative microradiographic study, Dent. Mater. 25 (2009) 884–891.
[42] K. Liang, M.D. Weir, X. Xie, L. Wang, M.A. Reynolds, J. Li, H.H. Xu, Dentin remineralization in acid challenge environment via PAMAM and calcium phosphate composite, Dent. Mater. 32 (2016) 1429–1440.
[43] M.D. Weir, L.C. Chow, H.H. Xu, Remineralization of demineralized enamel via calcium phosphate nanocomposite, J. Dent. Res. 91 (2012) 979–984.
[44] E.Y. Neres, M.D. Moda, E.K. Chiba, A. Briso, J.P. Pessan, T.C. Fagundes, Microhardness and roughness of infiltrated white spot lesions submitted to different challenges, Oper. Dent. 42 (2017) 428–435.
[45] B.W. Sigusch, T. Pflaum, A. Volpel, K. Gretsch, S. Hoy, D.C. Watts, K.D. Jandt, Resin-composite cytotoxicity varies with shade and irradiance, Dent. Mater. 28 (2012) 312–319.
[46] ISO, Standard, 10993-5, Part 5: Tests for in Vitro Cytotoxicity, Biological Evaluation of Medical Devices, ISO copyright office, Switzerland, 2009.
[47] F. Li, M.D. Weir, H.H. Xu, Effects of quaternary ammonium chain length on antibacterial bonding agents, J. Dent. Res. 92 (2013) 932–938.
[48] I.R. Reynolds, A review of direct orthodontic bonding, Br. J. Orthod. 2 (1975) 8.
[49] R.J. Scougall Vilchis, S. Yamamoto, N. Kitai, K. Yamamoto, Shear bond strength of orthodontic brackets bonded with different self-etching adhesives, Am. J. Orthod. Dentofacial Orthop. 136 (2009) 425–430.
[50] A.S. Altmann, F.M. Collares, V.C. Leitune, S.M. Samuel, The effect of antimicrobial agents on bond strength of orthodontic adhesives: a meta-analysis of in vitro studies, Orthod. Craniofac. Res. 19 (2016) 1–9.
[51] M.D. Weir, J.L. Moreau, E.D. Levine, H.E. Strassler, L.C. Chow, H.H. Xu, Nanocomposite containing CaF(2) nanoparticles: thermal cycling, wear and long-term water-aging, Dent. Mater. 28 (2012) 642–652.

[52] S. Rogers, B. Chadwick, E. Treasure, Fluoride-containing orthodontic adhesives and decalcification in patients with fixed appliances: a systematic review, Am. J. Orthod. Dentofacial Orthop. 138 (390) (2010) e391-390 e398.
[53] C. Dawes, What is the critical pH and why does a tooth dissolve in acid? J. Can. Dent. Assoc. 69 (2003) 722–724.
[54] N. Beyth, I. Yudovin-Farber, R. Bahir, A.J. Domb, E.I. Weiss, Antibacterial activity of dental composites containing quaternary ammonium polyethylenimine nanoparticles against Streptococcus mutans, Biomaterials 27 (2006) 3995–4002.
[55] X. Xu, Y. Wang, S. Liao, Z.T. Wen, Y. Fan, Synthesis and characterization of antibacterial dental monomers and composites, J Biomed Mater Res B Appl Biomater 100 (2012) 1151–1162.
[56] C. Van Loveren, Antimicrobial activity of fluoride and its in vivo importance: identification of research questions, Caries Res. 35 (Suppl 1) (2001) 65–70.
[57] D. Sardana, J. Zhang, M. Ekambaram, Y. Yang, C.P. McGrath, C.K.Y. Yiu, Effectiveness of professional fluorides against enamel white spot lesions during fixed orthodontic treatment: a systematic review and meta-analysis, J. Dent. 82 (2019) 1–10.
[58] Y. Liu, L. Zhang, L.N. Niu, T. Yu, H.H.K. Xu, M.D. Weir, T.W. Oates, F.R. Tay, J.H. Chen, Antibacterial and remineralizing orthodontic adhesive containing quaternary ammonium resin monomer and amorphous calcium phosphate nanoparticles, J. Dent. 72 (2018) 53–63.
[59] J.M. Ten Cate, In vitro studies on the effects of fluoride on de- and remineralization, J. Dent. Res. 69 (1990) 614–619.
[60] P.J. Milward, G.O. Adusei, C.D. Lynch, Improving some selected properties of dental polyacid-modified composite resins, Dent. Mater. 27 (2011) 997–1002.
[61] S. Lata, N.O. Varghese, J.M. Varughese, Remineralization potential of fluoride and amorphous calcium phosphate-casein phospho peptide on enamel lesions: an in vitro comparative evaluation, J. Conserv. Dent. 13 (2010) 42–46.
[62] H.B. Pan, B.W. Darvell, Solubility of calcium fluoride and fluorapatite by solid titration, Arch. Oral Biol. 52 (2007) 861–868.
[63] J.W. Nicholson, B. Czarnecka, The biocompatibility of resin-modified glass-ionomer cements for dentistry, Dent. Mater. 24 (2008) 1702–1708.
[64] L. Stanislawski, X. Daniau, A. Lauti, M. Goldberg, Factors responsible for pulp cell cytotoxicity induced by resin-modified glass ionomer cements, J. Biomed. Mater. Res. 48 (1999) 277–288.